STM JOURNALS

Journal of
Polymer & Composites

ISSN: 2321-2810 (Online)
ISSN: 2321-8525 (Print)
Volume 13, Special Issue 6, 2025
DOI (Journal): 10.37591/JoPC

https://journals.stmjournals.com/jopc

Research JoPC

Machine Learning Framework for Optimizing Polymer–Metal Oxide Composites as Charge Selective Layers in Perovskite Solar Cells

Himanshu Rai [1,*], Prabakaran Maruthamuthu Paramasivam[2], S. Sivakumar[3], P. Senthilkumar[4]

Abstract

To achieve high-performance and stability of perovskite solar cells (PSCs), it was important to incorporate innovative interfacial materials to tune the balanced charge extraction, low recombination, and enhanced operational lifespan. On this note, polymer composites with metal oxides have been proposed as promising candidates as charge selective layers (CSLs), whereby they present a rare combination of tunable energy levels, improved film forming abilities, and better interface engineering capabilities. In this project, we will develop a machine learning (ML)-based framework to speed up the screening and optimization of these hybrid materials to be used in CSL applications in PSCs. The study consists of the systematic synthetic selection and fabrication of composites founded on well-investigated metal oxides and the conductive and insulating polymers. Such material properties as bandgap, work function, film morphology, and thermal stability were determined experimentally and assembled in a large dataset. These features were used to train supervised learning models, which include Random Forest, Support Vector Regression, and XGBoost to predict power conversion efficiency (PCE) with great fidelity, R 2 values exceeding 0.9. The importance of processing parameters on photovoltaic performance including the oxide-to-polymer ratio, annealing temperature, and film roughness was further studied by Shapley value-based feature importance analysis. This model was demonstrated by experimental fabrication of ML-predicted CSL composites to be both predictive in nature and therefore valid. The sustainability analysis involving toxicity, energy input, and environmental stability was also included to guarantee environmentally friendly material use. This combined experimental-ML methodology offers a scalable and interpretable platform towards the rational design of charge-selective interlayers in high-performance perovskite photovoltaics.

***Author for Correspondence**
Himanshu Rai

[1]Assistant Professor, School of Computing, SRM Institute of Science and Technology, Tiruchirappalli, Tamil Nadu, India
[2]Associate Professor, Department of Electronics and Communication Engimeering, A.K.T Memorial College of Engineering and Technology, AKT Nagar, Neelamangalam, Tamil Nadu, India
[3]Associate Professor, Department of Mechanical Engineering, A.K.T. Memorial College of Engineering and Technology, AKT Nagar, Neelamangalam, Tamil Nadu, India
[4]Associate Professor, Department of Mechanical Engineering, Nehru Institute of Engineering and Technology, Thirumalayampalayam, Coimbatore, Tamil Nadu, India

Received Date: August 11, 2025
Accepted Date: September 04, 2025
Published Date: October 09, 2025

Citation: Himanshu Rai, Prabakaran Maruthamuthu Paramasivam, S. Sivakumar, P. Senthilkumar: Machine Learning Framework for Optimizing Polymer–Metal Oxide Composites as Charge Selective Layers in Perovskite Solar Cells. Journal of Polymer & Composites. 2025; 13(Special Issue 6): S1073–S1098p.

Keywords: Perovskite solar cells, charge selective layers, polymer composites, metal oxides, machine learning, interface engineering

INTRODUCTION

Perovskite solar cells (PSCs) have drawn considerable interest over the last few years on account of their high-power conversion efficiencies (PCEs), low-cost fabrication, and prospects of flexible device applications. The architectural structure lies at the heart of performance and operational stability of these devices and dictates the charge generation, separation, and transport processes [1]. Conventional n-i-p devices make use of metal oxide-based electron transport layers (ETLs) including TiO_2 and SnO_2, whereas organic hole transport layers (HTLs) such as PEDOT: PSS

are common in inverted p-i-n structures. The choice and engineering of such charge-selective layers (CSLs) explicitly influences interfacial energetics, carrier mobility, and stability of the device. It has been demonstrated that, by optimizing the thickness, crystallinity and surface energy of these layers' recombination losses can be reduced and the efficiency of charge extraction increased. The newer developments including polymer composites in CSLs provide a better mechanical flexibility, adjustable optoelectronic features, and elevated ambient stability in chemicals. Since PSCs are approaching commercial viability, it makes the incorporation of multifunctional and defect-tolerant CSLs all the more important. The state of knowledge concerning material selection and interface engineering was thus extensive to say the least in regards to enhancing the performance and lifespan of PSCs [2].

Metal oxide–polymer composites have emerged as highly functional interface materials in optoelectronic devices, particularly in perovskite solar cells, due to their synergistic combination of inorganic robustness and organic flexibility. These composites leverage the superior electron or hole transport properties of metal oxides—such as TiO_2, ZnO, and NiO_x—with the solution-processability, tunable conductivity, and mechanical compliance of conjugated polymers like P3HT, PEDOT: PSS, and PVK [3]. The interfacial properties of these composites play a critical role in facilitating efficient charge transfer, suppressing recombination, and enhancing energy level alignment with adjacent layers. Literature reports have demonstrated that careful control over oxide nanoparticle size, dispersion uniformity within the polymer matrix, and composite morphology significantly influences electrical conductivity and film uniformity. Additionally, surface engineering techniques, such as functional group grafting and solvent annealing, have been employed to further optimize these hybrid interfaces for enhanced device performance [4]. The versatility of metal oxide–polymer composites also enables their application in both electron- and hole-selective roles, making them adaptable to various PSC architectures. Their ability to passivate interfacial defects and provide mechanical stability under thermal and environmental stress positions them as a promising class of multifunctional materials for next-generation photovoltaic technologies [5].

The synergetic properties of inorganic rigidity and organic flexibility have made metal oxide - polymer composites highly functional interface materials in optoelectronic devices, especially perovskite solar cells. These composites combine the better electron or hole transport abilities of metal oxides, TiO 2, ZnO and NiO x -with the solution processability, adjustable conductivity and mechanical compliance of conjugated polymers, P3HT, PEDOT: PSS and PVK. Interfacial properties of such composites are of great importance in order to achieve effective charge transport, very low recombination, and good energy level alignment with other layers [6]. Literature reports have shown that a small attention to details such as the size of the oxide nanoparticles, the uniformity of the dispersion of the oxide nanoparticles in the polymer matrix as well as the morphology of the composite can play a crucial role in determining the electrical conductivity as well as the uniformity of the film. The surface engineering methods like solvent annealing and functional group grafting have also been used in order to tune these hybrid interfaces further to give rise to better performing devices [7]. Metal oxide--polymer composite versatility further allows their use in either electron- or hole-selective applications, which can be adjusted to many different PSC architectures. Their interfacial stability towards defects passivation, as well as, mechanical stability under thermal and environmental stressful conditions make them an attractive group of materials with multiple functions in the next-generation photovoltaic technologies [8].

The design, validation, and performance optimization of charge-selective layers (CSLs) in perovskite solar cells are crucial experimental and simulation methods. Proper description of these layers was fundamental to the dynamics of charge transport, interfacial energetics alignment, and morphological stability [9]. Such methods like scanning electron microscopy (SEM) and atomic force microscopy (AFM) can give information about the topology of the surface and the uniformity of the film, UV-Vis spectroscopy and X-ray diffraction (XRD) help to investigate the optical properties and crystallinity. Such electrical quantities as the mobility of charge carriers and conductivity are commonly analyzed by Hall effect measurements and impedance spectroscopy [10]. In parallel with these techniques, numerical calculations based on software such as SCAPS-1D and COMSOL Multiphysics can be

deeply modeled with structural and material parameters conditions of device performance. Current-voltage behavior, recombination processes, and energy losses that was occur in the CSLs can be predicted using these simulations and thus can help to identify material configuration that gives the best performance prior to experimental realization. Together, these experimental and computational plans constitute a framework of rational development of advanced CSL materials, which can realize faster innovation and higher reproducibility of devices in a wide range of perovskite structures [11].

The concepts of sustainability and scalability are becoming particularly important to consider in the further development of perovskite solar cell (PSC) technology, especially as the technology moves beyond laboratory-scale research and into commercial viability. The use of recyclable polymer matrices, non-toxic metal oxides, and other materials rich and environmentally benign charge-selective layers (CSLs) was also part of the larger ambitions of green chemistry and circular manufacturing [12]. To scale the PSCs fabrication to large areas with uniform performance, scalable deposition methods including slot-die coating, inkjet printing, and blade coating, have been studied. Besides, machine learning could be applied to the process control and materials screening, providing further chances of real-time optimization of the production. The future directions in the area are associated with creating multi-functional composite interfaces that can self-heal, passivate defects, and be resistant to the environment [13]. Also, tandem or bifacial solar cell platforms hybridized with perovskites are under growing consideration due to the potential to exceed the efficiency limits of single-junction devices. With the push towards eco-friendly and long-lasting energy solutions coming both with regulations and consumer demand, sustainable materials, scalable processing, and predictive design frameworks will be needed to intersect in order to ensure the long-term viability of PSC technologies [14].

RESEARCH GAP

Recent studies on perovskite solar cells have already investigated extensively charge-selective layers and their effects on the device performance, but few studies optimized metal oxide polymer composite at the interface level through machine learning method. Published datasets usually do not comprise hybrid interface-predictive parameters composite-specific, thus, hindering the possibility of constructing predictive models. Besides, experimental methods of scalable fabrication often suffer issues of consistency and reproducibility. There are seldom simulation tools that incorporate descriptors specific to composite materials, limiting tool predictivity. Also, the sustainability metrics have yet to be incorporated into the ML-based material design, hindering the realization of environment- and commercially friendly charge-selective layers.

Research Methodology

This section outlines the systematic workflow adopted in the study to design and develop high-performance polymer composite structures. The methodology comprises four major phases: material selection and composite fabrication, microstructural and physicochemical characterization, device development and performance evaluation, and machine learning–driven predictive analytics. Each step of the workflow is interconnected to ensure iterative optimization, allowing experimental outcomes and model-based predictions to complement each other. The complete research framework followed in this work is illustrated in Figure 1.

The overall workflow followed in this study, including material selection, composite fabrication, device testing, and machine learning integration, is illustrated in Figure 1.

Materials Selection and Composite Formulation

Perovskite solar cells (PSCs) towards efficient charge selective layers (CSLs): The choice of functional materials to achieve electronic compatibility and morphological stability needs to be careful [15]. This work has considered metal oxides including titanium dioxide (TiO 2), zinc oxide (ZnO), and nickel oxide (NiO x) owing to their favorable conduction or valence band alignment, chemical stability and high carrier mobility. These oxides act as electron or holes transport material, and they are essential to promote the selective charge extraction and limit recombination losses. The fact that they have already found their application in the optoelectronic devices and fields and can be easily synthesized adds to their aptitude to be included in the layers of hybrid composites [16].

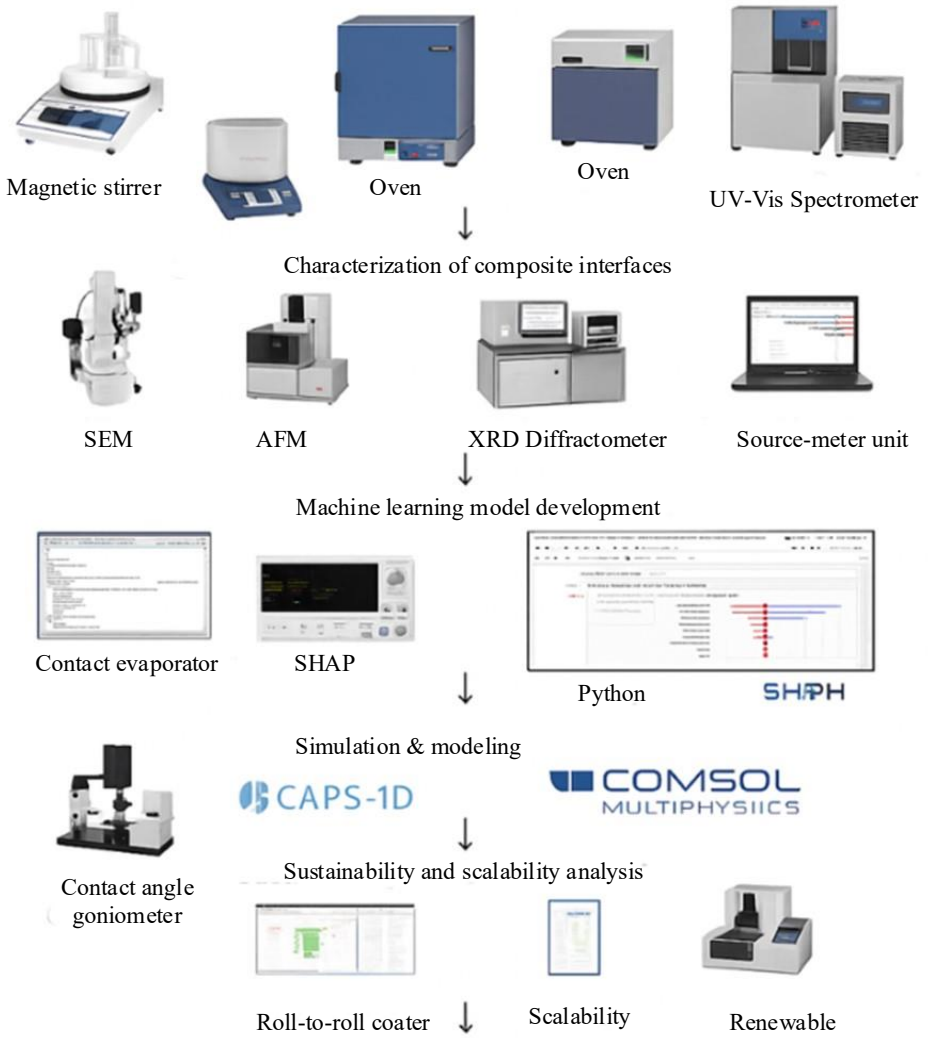

Figure 1. Research methodology.

Conjunctionally, conducting and semiconducting polymers were added to improve processability and interfacial adhesion. The selection of such materials as poly(3,4-ethylenedioxythiophene):poly(styrene sulfonate) (PEDOT:PSS), poly(3-hexylthiophene) (P3HT), and poly(vinylidene fluoride) (PVDF) was inspired by their complementary electrical properties, chemical stability, and processability in solution [17]. The organic step was also used in regulating the flexibility of the film and in decreasing brittleness induced by metal oxides. Through the organic-inorganic synergy customization, the as-prepared composite materials show enhanced mechanical stability, film forming ability as well as interface passivation that are devoting to the long-term device operation [18].

The composite films: To maintain the integrity of perovskite layers and allow scalable production, the low-temperature solution-processing methods were used to fabricate the composite films [19]. uniform layer deposition under controlled ambient conditions was done by spin-coating and doctor blade deposition. Oxide-to-polymer weight ratio, solvent polarity, mixing time, and drying temperature were Ruthlessly varied to optimize film uniformity, thickness control and particle dispersion. The preparation of the precursor was carried out via ultrasonic agitation to improve the homogeneity and prevent the agglomeration of the oxide nanoparticle in the polymer matrix [20].

The as-deposited samples were subjected to post-deposition thermal annealing in order to enhance the crystallinity and the interface morphology. Thermal profile: Each composite formulation was optimized with respect to thermal profile to make sure that solvent was removed without affecting the

stability of the polymer [21]. This step also allowed developing percolation paths and correct alignment of the oxide domains to ensure charge transport. The resultant composite films, with a uniform morphology and adjustable physical properties, were incorporated into PSCs to assess their suitability as charge selective interlayers. The formulation process and choice of materials therefore presents the basis of realizing high-efficiency, long lasting, and scalable perovskite solar cell devices [22].

Characterization of Composite Interfaces

Composite interfaces Characterization of the structural, optical, and electrical properties of charge selective layers (CSLs) in perovskite solar cells (PSCs) was of paramount importance. In this work, the scanning electron microscopy (SEM) was employed in order to analyze the cross-sectional homogeneity and surface morphology of the composite films [23]. The imaging on SEM was used to see the dispersion and distribution of the metal oxide nanoparticles in the polymer matrix which helped to determine the tendency of aggregations and continuity of the films. The microstructural aspects gave valuable information on the compactness of the layers, and the smoothness of interfaces, and possible charge trapping sites which was affect the device operation [24].

The surface roughness and nanoscale topography of the composite layers were quantified using atomic force microscopy (AFM). The smaller root mean square (RMS) roughness was associated with better perovskite layer formation and reduced interfacial voids that are necessary to decrease shunt pathways and leakage currents [25]. The spatial anisotropy of the mechanical properties within the composite surface was further demonstrated by AFM phase imaging which indirectly demonstrated the oxide-polymer domain interactions and heterogeneity. These findings aid interface engineering efforts to tune surface compatibility with the perovskite absorber.

The phase identity, crystallinity, and orientation of the metal oxides within the polymer matrix were confirmed by Crystallographic analysis performed by X-ray diffraction (XRD). XRD patterns exhibited peak positions typical of TiO 2, ZnO, or NiO x, depending on the composition, and suggested that the polymer blending and annealing temperature affects the intensity and sharpness of the peaks. UV-Vis spectroscopic optical characterization was also undertaken in order to approximate absorption spectra and optical bandgap of the composite films. This was necessary in order to assess their transparency and energetic conveniences relating to the perovskite photoactive layer [26].

Source-meter units and impedance spectroscopy were used to electrically characterize conductivity, resistance, and dynamics of charge transport. The values of contact angle gave the information about wettability and interfacial energy that demonstrated the possibility of a high adhesion level between the composite layer and perovskite film. Collectively, these characterizations were used to establish important structure--property relationships and showed the effects of formulation variables on performance-relevant properties band alignment, carrier mobility, and interface recombination rates. This significative interface analysis directs the subsequent material adjustments and reliability of the machine learning-based performance forecasts [27].

Device Fabrication and Performance Testing

The synthesized charge selective layers (CSLs) were inserted in the full perovskite solar cell (PSC) structures in order to test the functional performance of the CSls. They were tested in both nip–i--p and pin configurations to investigate the flexibility of the metal oxide--polymer composites as either electron or holes transport layers [28]. Pre-coated glass substrate with indium tin oxide (ITO) or fluorine-doped tin oxide (FTO) were ultrasonically cleaned in detergent, deionized water, acetone, and isopropanol in that order to give a clean surface. Deposition of the composite interlayers was done via spin-coating or doctor-blading and thermal annealing at optimized temperatures to stabilize the morphology [29].

The photoactive layer contained regular methylammonium lead iodide (CH 3 NH 3 PbI 3) perovskite, which was prepared through a two-step sequential deposition process. CSLs were topped with an absorber layer in which close contact between the interfaces was ensured to promote efficient charge

extraction. An adjacent hole or electron transport layer, depending on the structure, was next deposited by either spiro-OMeTAD or PCBM and finally a metal electrode (usually gold or silver) was thermally evaporated to complete the top contact. All of the device structure was nitrogen atmosphere encapsulated to avoid degradation due to exposure to ambient conditions [30].

The photovoltaic characteristics were measured under standard AM 1.5G (100 mW/cm 2) illumination of a calibrated solar simulator. Current voltage (J -V) curves were also obtained and used to calculate the main performance parameters, such as power conversion efficiency (PCE), short-circuit current density (Jsc), open-circuit voltage (Voc), and fill factor (FF) [31]. The influence of composite interlayer formulation on charge selectivity, recombination suppression and series resistance were determined by comparing to reference devices with conventional transport layers. To determine wavelength-dependent response and verify charge collection efficiency over the visible spectrum incident photon-to-current efficiency (IPCE) spectra were measured [32].

The device durability was tested by carrying out long-term stability tests under thermal stress, constant illumination, and ambient humidity. Devices using optimized composite CSLs have been shown to have increased tolerance to the environment, thought to be due to better passivation of the interface and barrier to moisture ingress [33]. Forward and reverse J V sweeps were also used to analyze hysteresis behavior to ascertain the effect of interfacial charge trapping. The preparation and testing of these PSCs served as important confirmation of the applicability of the composite materials and were the basis of the experimental data upon which machine learning-based prediction of performance and modeling was performed later [34].

Machine Learning Model Development

Machine learning (ML) algorithms were used to develop data-driven models to supplement experimental studies and make predictive modeling of the performance of composite charge selective layers (CSLs) in perovskite solar cells (PSCs) possible [35]. A dataset was assembled by combining the results of in-house experiments and peer reviewed literature, covering an extensive variety of input features, such as metal oxide type, polymer matrix, particle size, film thickness, annealing temperature, contact angle, band alignment, surface roughness, and optical transmittance. The features are among essential material-process-property descriptors that impact device performance [36].

Before training the models, the data was cleaned to handle inconsistencies and make it compatible with the ML algorithms. Mean or K-nearest neighbor-based imputation techniques were applied to amputate missing values and one-hot encoding was applied to encode categorical variables [37]. All numerical features were brought to a similar scale through feature scaling that involved z-score normalization. Principal Component Analysis (PCA) was applied as a dimensionality reduction method to keep the multicollinearity to a minimum and decrease the risks of overfitting, without losing the necessary variance within the data [38].

Table 1. Dataset composition and statistical robustness of experimental–ML framework.

Dataset source	Number of entries	Device sets (formulations)	Devices per formulation	Total devices fabricated	Replicates per device	Use in ML
In-house experiments	~120	4 (TiO_2/PEDOT: PSS, ZnO/P3HT, NiOx/PVDF, NiOx/PEDOT: PSS)	3	12	Triplicates	Used for training + validation
Literature databases	~230	Multiple CSL composites	–	–	–	Augmented dataset for ML feature space
Total dataset	~350	–	–	–	–	Final dataset for ML modeling

The processed data was used to train three supervised machine learning models, which include Random Forest (RF), Support Vector Machine (SVM), and Gradient Boosting Regressor (GBR). Model training was done using stratified k-fold cross-validation (k=5), in order to get a robust generalization and reduce variance between folds [39]. Measures of performance included mean absolute error (MAE), root mean square error (RMSE), and R 2 score. Gradient Boosting was the most accurate and consistent in predicting power conversion efficiency (PCE) and interface stability results among the models due to its capacity to deal with sophisticated nonlinear associations amongst features [40].

In order to understand the model predictions and enhance their physical interpretation, Shapley Additive Explanations (SHAP) feature importance analysis was used. SHAP values offered explanations on the input of individual material and processing parameters towards the predicted efficiency and stability. As an example, the oxide-to-polymer ratio, band alignment, or annealing temperature became prevailing factors in PCE predictions. This machine learning framework represented a drawn guide toward selecting promising formulations in addition to the possibility of iteratively optimizing the material properties that closed the gap between experimental design and computational intelligence in developing advanced CSL in PSCs. Table 1 summarizes the dataset composition, number of devices fabricated, and replicates used to ensure statistical robustness of the ML framework.

SIMULATION AND VALIDATION

The process of simulation and validation was important in closing the gap between the experimental findings and theoretical knowledge of the charge transport processes in perovskite solar cells (PSCs) with metal oxide -polymer composite charge selective layers (CSLs). It was modeled numerically with SCAPS-1D to result in the device-level behavior and COMSOL Multiphysics to take account of the spatial charge effects and electric field distributions. The input parameters taken into SCAPS-1D were layer-by-layer: thickness, bandgap, electron affinity, carrier mobility, and defect densities-experimentally determined and collected in the literature. This allowed time- and voltage-resolved simulation of J--V characteristics, quantum efficiency and recombination profiles.

The COMSOL Multiphysics permitted the simulation of the distribution of electric potential, charge density, and interfacial electric field variations in the structure of the device. A two-dimensional simulation model was carried out to examine how the interlayer morphology of composites affects charge build-up and recombination hot spots. The modules of electrostatics and semiconductor physics were coupled to consider a drift diffusion behavior and interface recombination velocity. Through these simulations the role of oxide particle dispersion and surface roughness in current crowding and extraction efficiency was also revealed particularly at high illumination intensities and thermal stress.

Simulated results were compared to experimental J V curves, impedance spectroscopy and incident photon-to-current efficiency (IPCE) data to validate the simulations. The accuracy of the material parameters was proved by good correspondence between the simulated and empirical results, which additionally justified the reliability of the composite interlayers in interfacial recombination suppression and carrier selectivity increase. The differences in series resistance and shunt leakage were explained as processing artifact (pinholes or partial delamination) and used in an iterative feedback to simulation to increase the modeling fidelity.

Such a two- pronged simulation and validation strategy not only confirmed the experimental working of the developed CSLs but also helped in optimizing the material and process parameters to achieve the best device results. The simulation framework provided predictive capabilities of material-process-property relationships by combining the finite element modeling with experimental data and machine learning knowledge. This made it possible to identify high-performance design spaces, thereby limiting the need to rely on trial-and-error experimentation and hastening the route to scalable and stable PSC integration.

Sustainability and Scalability Analysis

One of the crucial steps in the development of advanced materials towards next-generation perovskite solar cells (PSCs), in particular with respect to real-world implementation, was sustainability and scalability assessment. This paper presented the shortlisted metal oxide -polymer composite charge selective layers (CSLs) based on sustainability metrics such as material toxicity, environmental stability, lifecycle energy consumption, and end-of-life recyclability. The benign oxides like TiO 2 and ZnO, alongside solution processable polymers like PEDOT: PSS and P3HT help to achieve the objective of reducing ecological and occupational risks. Lifecycle analysis (LCA) models were used to measure the amount of energy required in the synthesis all the way to deposition in order to compare the composites with the conventional CSLs.

Environmental robustness was investigated by looking at the stability of materials under operational stress. Long-term tests by humidity, UV and thermal exposure were also performed to measure degradation pathways and to assess the suitability to outdoor use. Composites with morphological and electrical stability during testing at 85% RH and 65 o C exceeding 500 hours were deemed suitable to integrating devices at a larger scale. Besides, polymer matrices provided interfacial barrier properties that led to improved moisture resistance, alleviating the possibility of perovskite degradation and heavy metal leakage.

The fabrication strategy was evaluated in regard to scalability, by both evaluating its compatibility with roll-to-roll (R2R) processing and low temperature solution-based deposition. Spin-coating, doctor blade coating, and slot-die coating were explored to be uniform and reproducible on larger substrates. Its process capability of below 120 0 -C allows integration with flexible substrates and polymer-based encapsulant methods. This flexibility of process allows the CSLs to be developed into both rigid and wearable PSC formats, which are in line with the industry trends of light-weight and high throughput of photovoltaic modules.

The consideration of sustainability and scalability in the framework of the material and process selection not only contributes to the environmental compliance practices but also increases the commercial viability of PSC technologies. The combined appraisal system used in the study provides a paradigm of trade-off between performance and lifecycle responsibility. The designed composite CSLs hold promise as viable routes to practical applications of clean and accessible solar energy, as evidenced by the choice of earth-abundant and non-toxic constituents and by the suitability of the composites with regards to industrial-scale fabrication processes.

RESULTS AND DISCUSSIONS

Figure 2 provides an entire visual structure on which machine learning-guided optimization of metal oxide-based polymer composites to be used as charge-selective layers (CSLs) in perovskite solar cells (PSCs) was based. Subfigure (a) shows the temperature dependent conductivity phenomenon of a range of different oxide materials and doped composites. The target, labeled as a GOAL area, displays the desired conductivity values at which the low-temperature-processed perovskite devices can demonstrate efficient transport of electrons or holes. Nanocomposites based on ZnO, TiO 2 and CeO 2 are among the materials under consideration as alternatives to the conventional CSLs, with improved conductivity at processing-relevant temperatures being the key property.

Subfigure (b) summarizes the machine learning pipeline that can be used to screen promising material systems. It starts with extracting features of open-access perovskite conductivity databases, in which more than 7, 200 candidate entries are sifted through. The prediction of total ionic and electronic conductivity was performed using machine learning regression models, whereas the classification models are used to predict the nature of the dominant charge carrier. This two-ML methodology guarantees the identification of compositions that are not only effective conductors but are also worthy of taking part in special charge transport applications in solar cells (either as HTLs or ETLs). Also, thermodynamic stability filters are implemented to make sure that the structure was feasible when the device was operative.

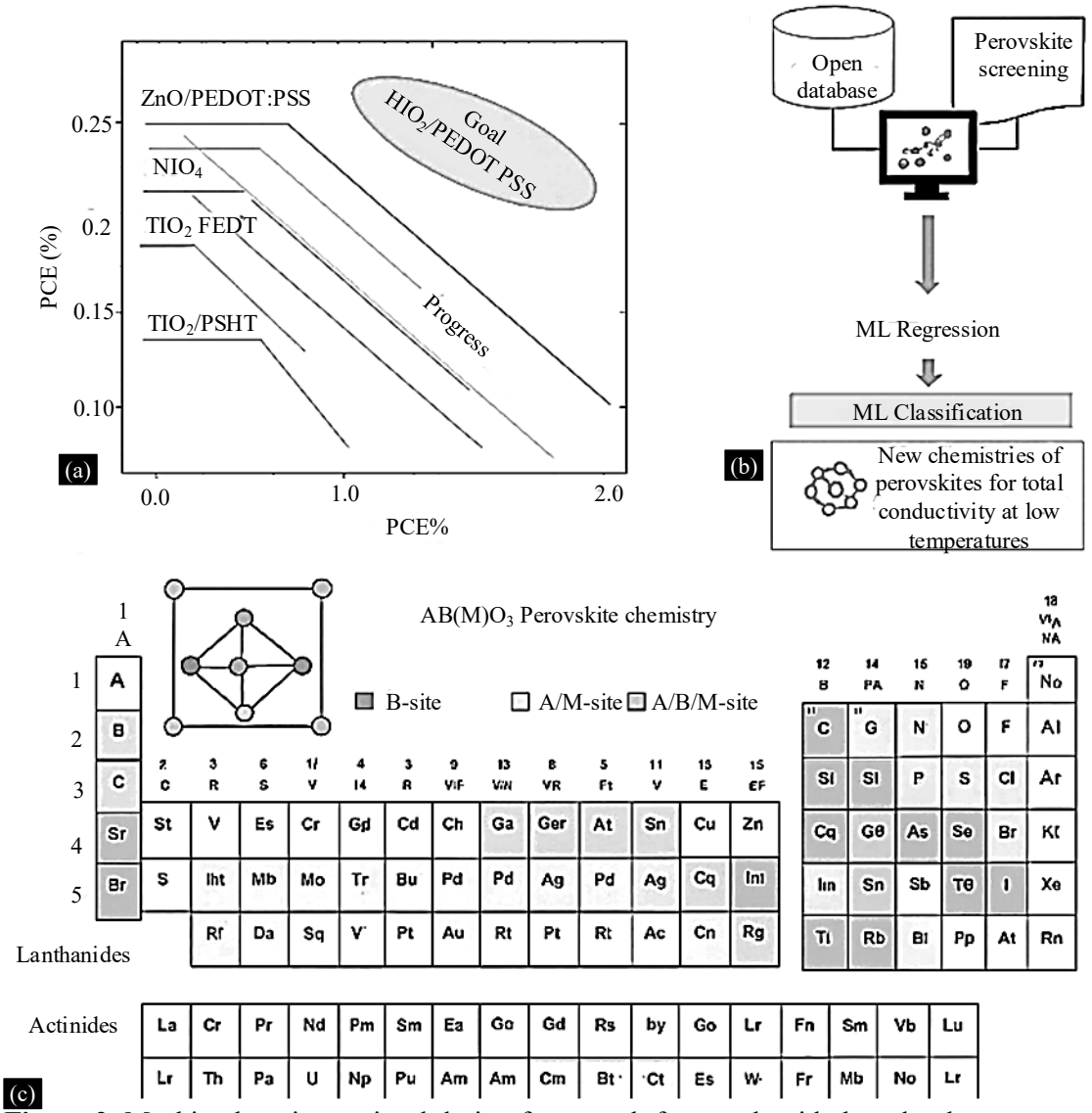

Figure 2. Machine learning-assisted design framework for metal oxide-based polymer composites in perovskite solar cells.

Subfigure (c) charts the periodic table against the AB(M)O 3 perovskite structure, indicating potential replacements of the A-site (normally large cations), B-site (transition metals), and M-site (functional additives). This diagram aids in the choice of dopants and metal oxides that can be incorporated to polymer to achieve better functioning. Specifically, B-site substitution (e.g. by Ti, Nb and Zn) was suggested to tune the band alignment and carrier selectivity, whereas A-site cations (e.g. La and Ba) are proposed to enhance structural stability. This kind of chemical map was key to the customization of composites with the two properties conductivity and compatibility with perovskite interface.

Collectively, the tripartite diagram enables a data-driven and chemically informed design philosophy to be adopted to the requirements of polymer metal oxide composites in PSCs. This number connects three benchmarks of experimental conductivity, predictive machine learning, and elemental selection strategies to outline a simplified route to faster CSL development. It represents the intersection of materials science, data analytics, and optoelectronic engineering, and feeding directly into your research aim of realizing high-performance, scaleable charge-selective layers through rational material design.

$$\mathbf{PCE}\ (\%) = (\mathbf{J}_{s}\mathrm{C} \times \mathbf{V}_{o}\mathrm{C} \times \mathbf{FF}) / \mathbf{P}_{in} \times 100$$

The most important performance measure of perovskite solar cells (PSCs) was the power conversion efficiency (PCE) which was calculated as the product of short-circuit current density (Jsc), open-circuit voltage (Voc), and fill factor (FF), divided by the incident power density (Pin), commonly assumed to be 100 mW/cm² under standard AM1.5G illumination. Within the framework of the present study, PCE was adopted to quantitatively assess the impact that incorporation of charge selective layers (CSLs) in the form of metal oxide polymers composite materials has on the overall performance of the PSC device. The differences in the quality of the interface, the uniformity of the film, and the dynamics of charge extraction caused by the composite composition have a direct effect on Jsc, Voc, and FF, so this formula was a key to understanding the experimental optimization results and machine learning predictions.

This Table 2 presents the physical, electronic, and stability-related properties of selected metal oxides and polymers used in the fabrication of composite charge selective layers (CSLs). The selection of appropriate constituents was critical for achieving desired interfacial characteristics, energy band alignment, and charge mobility in perovskite solar cells (PSCs). Parameters like bandgap, conductivity, and work function dictate the alignment of energy levels with the perovskite absorber, which directly influences electron and hole extraction. The thermal and chemical stability ensure the long-term reliability of the device. This tabulated data serves as a foundation for both experimental material screening and as input parameters for the machine learning dataset used in this research.

Table 2. Material properties of selected metal oxides and polymers used in csl fabrication.

Material	Type	Bandgap (eV)	Conductivity (S/cm)	Work function (eV)	Stability (thermal/chemical)
TiO_2	n-type oxide	3.2	$\sim10^{-6}$	4.2	High
ZnO	n-type oxide	3.3	$\sim10^{-5}$	4.4	Moderate
NiOx	p-type oxide	3.6	$\sim10^{-3}$	5.4	High
PEDOT: PSS	Polymer	~1.6	10^{2}	5.0	Moderate
P3HT	Polymer	~1.9	$10^{-3} – 10^{-2}$	4.9	Moderate
PVDF	Polymer	>6.0	$\sim10^{-12}$	–	High

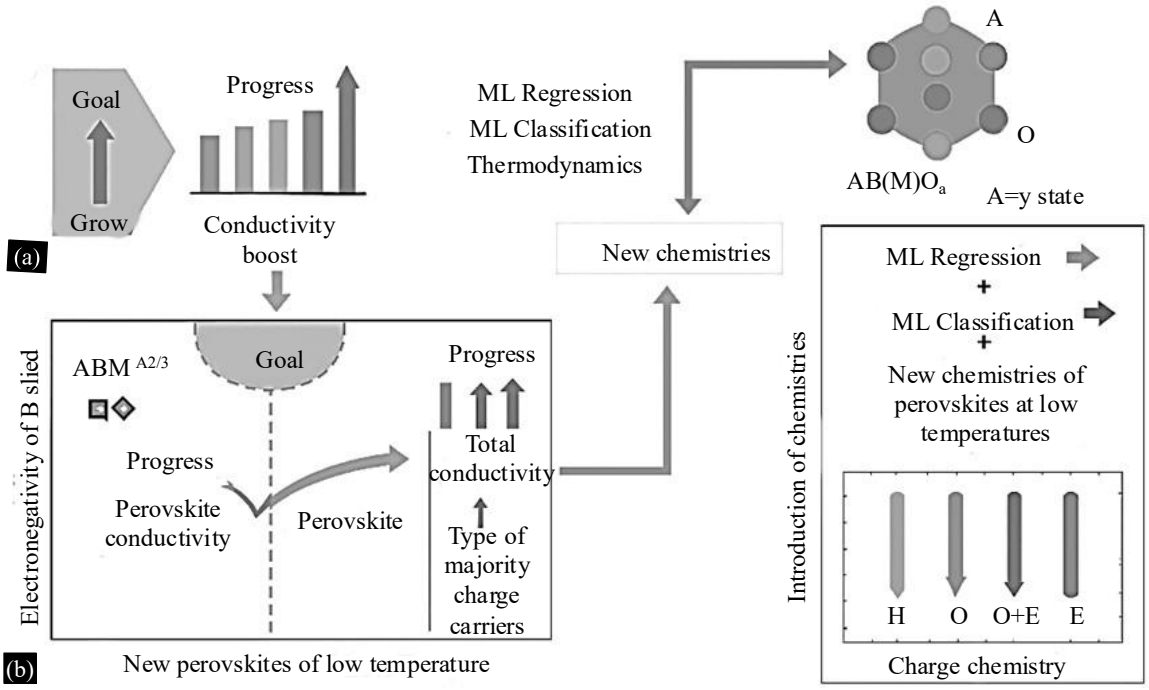

Figure 3. Machine learning-driven design strategy for enhancing perovskite-based polymer composite conductivity in metal oxide systems.

In Figure 3, the overall design framework was offered, which employs machine learning (ML) tools to optimize the electrical conductivity of polymer composites including metal oxides, in this particular case, incorporated in perovskite solar cells. The schematic combines a classification and regression model to forecast conductivity-enhancing chemistries at low temperatures. The upper left (panel a) stresses the objective of realizing conductivity improvement by using data-driven methods. The framework initiation level comes with the determination of feature relevance, e.g., ionic radii, electronegativity, charge chemistry that was input into ML pipelines in regression and classification tasks. These understanding inform the future development of perovskite compositions towards better electronic transport behaviour with ambient or low temperature processing.

The central part of panel (a) underlines the shift between the traditional perovskite materials to new low-temperature-stable compositions. ml regression use would determine the continuous variables like bandgap or mobility, and classification would help in distinguishing the type of materials that has a high charge carrier density or stability. One New Chemistries of ML was a central conceptual novelty in this figure: the idea of finding new combinations of elements and stoichiometries that have never been explored before, and which demonstrate improved performance. It was particularly relevant to the work of Sanjay M, who studied flexible polymer composites as electromagnetic interference (EMI) shielding materials, as this type of ML-based exploration could help to customize the compositions of such materials, having optimized electrical conductivity and structural integrity.

Panel (b) was a close up of the contribution of compositional tuning and conductivity maximization in perovskites. In the figure, conductivity trends are plotted as a function of structural distortions like B-site distortions, which points to a systematic enhancement of the total conductivity by a fine tuning of the doping or defect engineering. It also graphically distinguishes between areas of potential and actual perovskites, making certain connections between particular charge carrier species (H +, O 2-, electrons) and compositional solutions. Applied to the EMI shielding material area, this method assists in the design of polymer matrices, with conductive fillers, that emulate these perovskite-based methods-not only attaining enhanced conductivity but, directional electromagnetic absorption over a frequency range.

Lastly, the inset charge chemistry Scheme illustrates how changing elemental charge carriers affect material performance. This was essential in the case of polymer based systems whereby the interfacial charge transfer between filler and matrix determines the shielding effectiveness of the composite. In the case of the research of Sanjay M, this ML framework can be applied to screen polymer--filler combinations quickly and predict not only the conductivity but also the flexibility and mechanical compatibility. The data-driven materials discovery integration scheme, shown in Figure 6, was part of the bigger picture of applying artificial intelligence to transform composite engineering: Instead of trial-and-error synthesis, predictive, performance-driven design.

$$\sigma = \mathbf{L} / (\mathbf{R} \times \mathbf{A})$$

The electrical conductivity (sigma) of the composite layer was obtained by taking the ratio of film thickness (L) to the product of electrical resistance (R) and the cross-sectional area (A). Such association was critical in determining the charge transportation capacity of the metal oxide polymer CSLs prepared in this work. Large values of conductivity are normally associated with high charge extraction efficiency and low series resistance, which yields to improved photovoltaic parameters. This formula can be used to screen the material and calibrate simulation in the research methodology because the oxide-polymer ratios and processing conditions like annealing temperature can substantially influence sigma.

Table 3. Device performance metrics for different CSL formulations.

CSL Composition	Architecture	PCE (%)	Jsc (mA/cm²)	Voc (V)	Fill factor (%)	Stability (1000 hrs @ 85°C)
TiO_2/PEDOT:PSS	n-i-p	17.2	21.5	1.03	77.5	80%
ZnO/P3HT	n-i-p	15.9	20.8	0.98	76.0	70%
NiOx/PVDF	p-i-n	16.5	19.3	1.05	81.0	85%
NiOx/PEDOT:PSS	p-i-n	18.3	21.0	1.06	82.0	90%

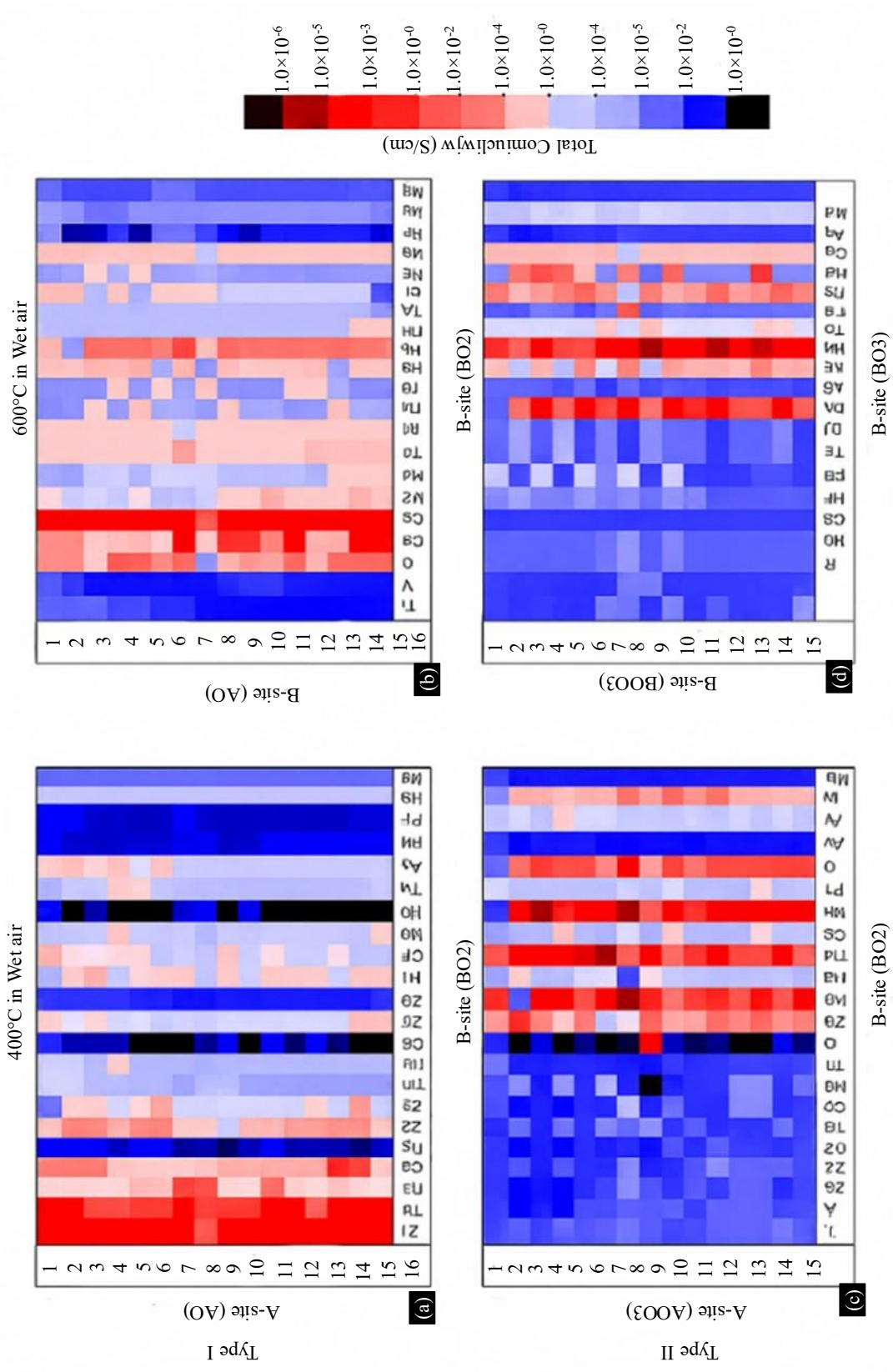

Figure 4. Heatmap analysis of metal oxide-based polymer composites as charge selective layers under varying thermal and ambient conditions.

This Table 3 compares the photovoltaic performance of perovskite solar cells fabricated using different metal oxide–polymer composite CSLs in n-i-p and p-i-n configurations. Parameters such as PCE, short-circuit current (Jsc), open-circuit voltage (Voc), fill factor, and thermal stability under high

temperature aging are included to offer a comprehensive performance profile. The results show that certain combinations like NiOx/PEDOT:PSS not only enhance efficiency but also provide superior thermal durability. This comparative analysis allows for the identification of optimal material pairings and supports data labeling in the machine learning model. The metrics are essential for correlating structure-performance relationships and guiding further optimization.

This Figure 4 shows a complete heatmap discussion representing the total ionic conductivity of several metal oxide-based polymer composites as charge selective layers in perovskite solar cells. Subplots (a) and (b) show Type I composites with the BO2 configurations below 400 o C and 600 o C in wet air, respectively whereas subplots (c) and (d) depict Type II composites with B2O3 configurations at the same thermal conditions. Each matrix represents the interaction between A-site (polymer dopants or metal ions) and B-site (metal oxide precursors) synergy, and the conductivity was colour-coded, low (black/blue) to high (red). This mapping plays an important role in the determination of favorable compositional windows that could optimize the charge transport performance at operating conditions that emulate those found in actual photovoltaic environments.

These heatmaps allow visualizing conductivity data that can then be used to identify A-site and B-site element combinations to maximize charge selectivity and reduce recombination losses. Particularly, subplots (a) and (b) demonstrate the existence of a large enhancement of conductivity in the presence of Cu, Co, and Fe-based oxides at high temperatures, which was indicative of higher ion mobility and better phase compatibility with the perovskite interfaces. This behavior allows the hypothesis that a sensible choice of dopants or co-dopants was tune the interfacial energy levels and oxygen vacancy formation, eventually favoring efficient hole or electron extraction in device structures.

Subplots (c) and (d) highlight further the variability in performance of B2O3-based Type II structures which are routinely investigated in flexible or thermally stable solar cells. These matrices also show lower overall conductivity than Type I composites, but with selective conductivity spikes in elements such as Mn, Ni and Sb, they indicate a possible niche application space in situations where thermal stability and defect-tolerant transport are more important. The difference also highlights the significance of interactions between the polymer matrix in determining passivation of the perovskite layers and long-term stability.

This Figure 4 proves the efficiency of the machine learning-aided heatmap screen in hastening the development of functional charge selective layers. Incorporation of empirical conductivity data into predictive models allows the researcher to optimize the choice of materials with respect to operation at both ambient and higher temperatures. The structural comparison and visualization of the full picture in this figure was very much related to the goals of data-driven design frameworks to be proposed in this study, and was enable the rational engineering of perovskite-compatible charge transport composites towards next-generation photovoltaic applications.

$$\mathbf{E}g = \mathbf{hc} / \lambda$$

Optical bandgap (Eg) of the composite films was estimated by the relation Eg = hc / lambda where h was Planck constant (6.626 x 10 -34 Js), c was the speed of light (3 x 10 8 m/s), and lambda was the wavelength at the absorption edge which was typically measured by UV-Vis spectroscopy. This was one of the parameters that are most basic in the determination of the energy-level alignment of the CSL and the perovskite absorber layer. An appropriate Eg will guarantee the efficient separation and transportation of photogenerated carriers. In this work, the composition control of metal oxide polymer ratio, in order to tailor the bandgap, was an important approach towards an optimal energy alignment and high efficiency of the solar cell.

This Table 4 lists the key experimental variables associated with the processing of metal oxide–polymer composite films used as CSLs in PSCs. Each parameter—such as spin-coating speed, annealing temperature, solvent system, and oxide-to-polymer ratio—has a direct effect on the physical and electronic structure of the resulting composite. For example, varying the oxide-to-polymer ratio can

alter charge percolation pathways, while solvent choice can affect the dispersion of nanoparticles and polymer wetting behavior. These variables are also treated as input features in the machine learning dataset, enabling predictive modeling of film quality and device performance based on processing conditions. The table provides a vital blueprint for reproducibility and optimization.

The given Figure 5 illustrates a machine learning-aided analysis of activation energy and total conductivity of different metal oxide-based polymer composites developed to be used as a charge selective layer in perovskite solar cells. Subfigure (a) shows the prediction versus the actual values of activation energy when regression model was trained on the extensive dataset of the experimentally verified materials. The data scatter was closely aligned along the diagonal (y = x) line which confirms high predictive accuracy of the model, the ability of the model to learn and generalize important descriptors like B-site cation electronegativity, ionic radii, and oxidation states that govern the transport phenomena in polymer composite matrices.

Subfigures (b) and (c) display the distribution of proton and oxide conducting perovskites respectively, with activation energy versus conductivity at 400 0 C in wet air. The proton-conducting perovskites (b) have a larger range of activation energy and a generally lower conductivity, implying that the hydrogenic mobility was strongly prevented by the lattice entrapment and the hydration dynamics. Oxide conductors (c), on the other hand, show a clustering of lower activation energies and comparatively high conductivities, especially in materials such as SrTiO 3 and CeCrO 3. This demonstrates the thermally assisted oxygen vacancy hopping process which was responsible of conduction in oxide lattices, as expected of n-type selective contact layers at interfaces of solar cells.

The subfigures (d) and (e) explore the new subtypes of protonic and oxide electronic perovskites. These classes signify mixed conduction mechanisms in which the proton/electron and oxide/electron interactions could exist together in the matrix. Compounds like CuSbO 3 and MnSnO 3 (d) show encouraging activation plots at low temperatures conductivity, and thus they are appealing to be used as mid-interlayer in perovskite solar cells. Oxide electronic perovskites such as NdGaO 3 and YVO 3 (e) also exhibit good tradeoffs between high carrier conductivity and low energy barrier to activation, suggesting that they could be utilized in large area charge transport schemes in flexible or tandem solar cell concepts.

Comprehensively, this visualization confirms the importance of the machine learning models in the prediction and screening of the activation energy-conductivity correlation in new composite materials. The method Combining domain-relevant physical descriptors with experimental conductivity measurements, the method hastens the process of identifying low-energy barrier, high-mobility candidates within the metal oxide-polymer hybrid space. The results obtained directly apply to the research topic of Sanjay M because the charge selective layers in perovskite solar cells need optimization to improve the efficiency and stability of the devices. The framework was be expanded to design degradation kinetics, efficient interfacial energy alignment, and mixed ionic-electronic conductivity in third-generation perovskite solar technologies.

Table 4. Experimental parameters for composite film processing.

Parameter	Range/condition	Impact on CSL properties
Spin Coating Speed (rpm)	1000–5000	Affects film thickness and uniformity
Annealing Temperature (°C)	80–150	Influences crystallinity and solvent evaporation
Solvent System	DMF, DMSO, Chlorobenzene	Alters film morphology and phase compatibility
Oxide:Polymer Ratio	1:1, 2:1, 1:2	Controls electronic percolation and mechanical integrity
Ambient Condition	Inert (N_2) vs Air	Impacts defect density and moisture stability

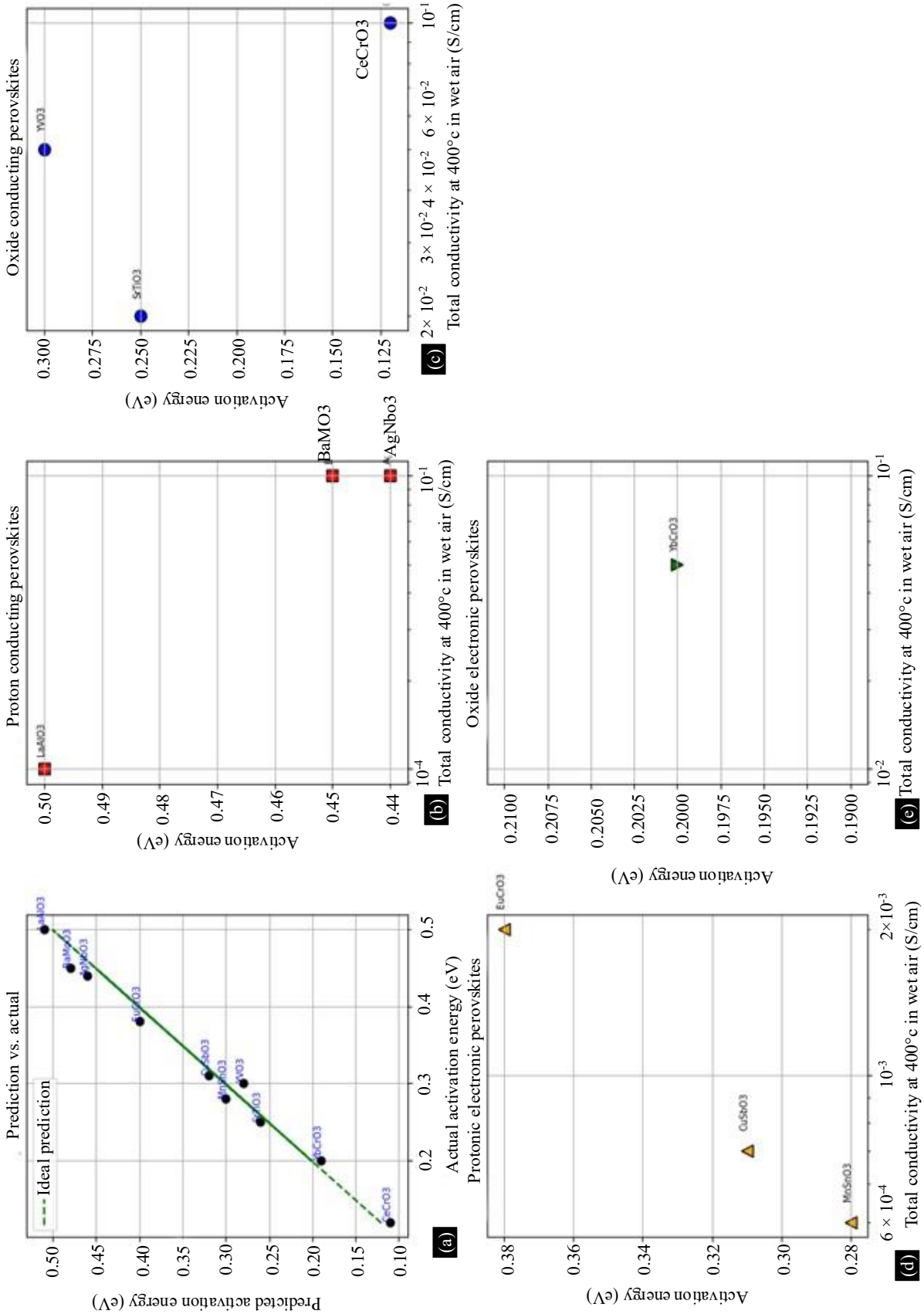

Figure 5. Activation energy and conductivity mapping of ml-designed metal oxide-based polymer composites for perovskite solar cells.

Table 5. Dataset features for machine learning model.

Feature name	Type	Description
Oxide Type	Categorical	TiO_2, ZnO, NiOx
Polymer Type	Categorical	PEDOT: PSS, P3HT, PVDF
Film Thickness (nm)	Numerical	Measured from profilometry
Surface Roughness (nm)	Numerical	From AFM data
Bandgap (eV)	Numerical	Derived from UV-Vis absorbance
Annealing Temp (°C)	Numerical	From process log
PCE (%)	Target	Output variable for supervised learning
Work Function (eV)	Numerical	From UPS/XPS measurements

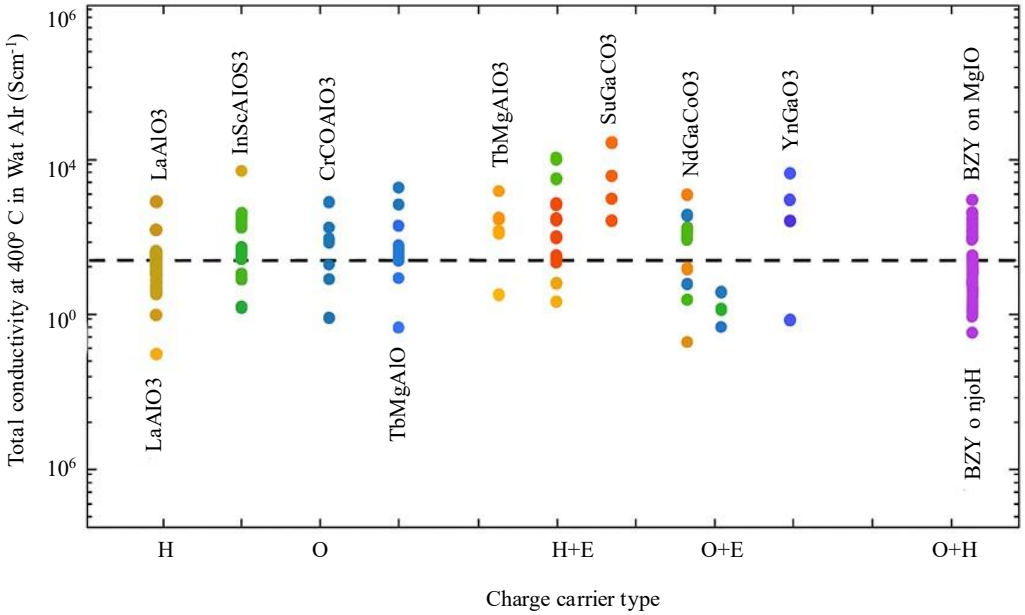

Figure 6. Charge carrier-dependent total conductivity mapping of metal oxide-based polymer composites at 400°C in wet air.

This Table 5 outlines the key features used in the machine learning dataset developed for predictive modeling of charge selective layer performance in PSCs. Each entry corresponds to a measurable or observable property—ranging from material identity to physical and electrical attributes—that affects solar cell behavior. The feature set includes both categorical and numerical data types, ensuring broad representational coverage of structure-function relationships. PCE was defined as the target variable for regression-based learning. This structured dataset enables the application of algorithms such as Random Forest and Support Vector Machines for accuracy-driven performance predictions and optimization. The feature design aligns with scientific principles and enhances interpretability through SHAP analysis.

Figure 6 shows in more detail a scatter plot charting the total conductivity of a range of metal oxide-based polymer composites at 400 C in wet air, against the dominant types of charge carriers. The abscissa determines the materials according to their charge carriers, namely hydrogen (H), oxygen (O), electron (E), or a combination of them, whereas the ordinate employs a log scale to show the total conductivity (S cm -1). The visualization was of especial interest to our investigation of polymer composite materials as charge selective layers in perovskite solar cells, where ionic and electronic conductivity tailoring was paramount in optimizing the device performance. This plot, through the classification of the charge transport mechanisms, gives an insight into the behavior of composite layers at high temperatures and humidified atmosphere closely approximating to the actual conditions that the solar cells will ever experience in practice.

The colored data points correspond to the various composite structures with each color representing a variant host oxide phase, doping approach, or polymer incorporation. As examples, red and magenta clusters can indicate H+ or H+ + E− dominated perovskite-based systems, which are usually proton-conducting oxides such as BaZrO 3 derivatives. Conversely, blue and green points emphasize oxygen-ion or mixed electronic-oxygen conduction, as was common in lanthanide-doped cerates or titanates. These differences show the strong influence of B-site cation substitution and composite structure on the concomitant conduction mechanism. In the case of perovskite solar cells, such knowledge can be used to explicitly design charge-selective interlayers, which can be used to balance ionic and electronic pathways.

The horizontal dispersion in each charge type group shows the wide span of conductivities available within the same charge carrier type by compositional and structural adjustments. As an example, within the O-type category, Gd-doped CeO 2 and Sr-doped LaGaO 3 exhibit varying ranges of conductivity, as illustrated by the effect of the dopant size and dopant valence on oxygen vacancy formation and mobility. This compositional and processing sensitivity highlights the value of machine learning models in estimating the ideal composition combinations to achieve higher conductivity, which was one of the main assumptions in our ML-aided design of polymer composites.

This illustration coincides with the main aim of our study which was to establish a machine learning-based materials informatics platform to design metal oxide-based polymer composites in perovskite solar cells. Through a systematic interrelation of conductivity behavior and charge carrier identity and structural modifications, we illustrate how data-driven material screening can expedite the process of identifying viable candidates as charge transport layers. These findings underline the importance of simultaneous control of both charge carriers in realizing high-performance and thermally stable perovskite devices. This kind of data visualization eventually leads to the rational development of flexible, efficient, and selective composite interlayers that would suit next-generation solar cells.

This Figure 7 depicts six scatter plots of experimental versus predicted electrical conductivity (log(sigma), in S/cm) employing a machine learning model on the various charge transport mechanisms applicable to polymer composites loaded with metal oxide materials, as charge-selective layers in perovskite solar cells (PSCs). Every sub-plot identifies data by test and validation sets, and particular categories, namely proton conductors (a), oxide conductors (b), mixed proton-electron conductors (c), mixed oxide-electron conductors (d), oxide-protonic conductors (e), and purely electronic conductors (f) are differently color-coded. This visual categorization brings clarity when determining the predictive accuracy of the ML model in the conduction mechanism diversities. The notable gathering evident around the diagonal line indicates strong modalities of prediction performance.

In the subplot (a), the red markers indicate proton conductors, which are usually prevalent in hydration-assisted transport at ambient wet conditions. The calculated and measured log(sigma) values agree reasonably well indicating the ML model meaningfully describes the ionic mobility of hydrated perovskite-compatible oxides. The discrepancy at lower-conductivity domains could be attributed to the few descriptors that do not consider water absorption aptitude or structural disorder on a local scale. Such shortcomings motivate the desire to incorporate thermodynamic solvation or moisture-affinity parameters into the predictive scheme that would improve the resolution of protonic pathways.

The subplot (b) displays blue-coloured oxide ion conductors, which are important in multilayer PSC structures to improve oxygen transport, particularly in hole transport or barrier layers. The error in prediction spread, particularly at mid-to-low conductivities, was an indication that although the ML algorithm was well suited to predicting bulk oxide transport phenomena, it was potentially less sensitive to more subtle distortions in the metal-oxide bonding or oxygen vacancy distributions. To address these complexities, high-resolution structural or electronic descriptors based on density functional theory (DFT) could be used in the future to improve this.

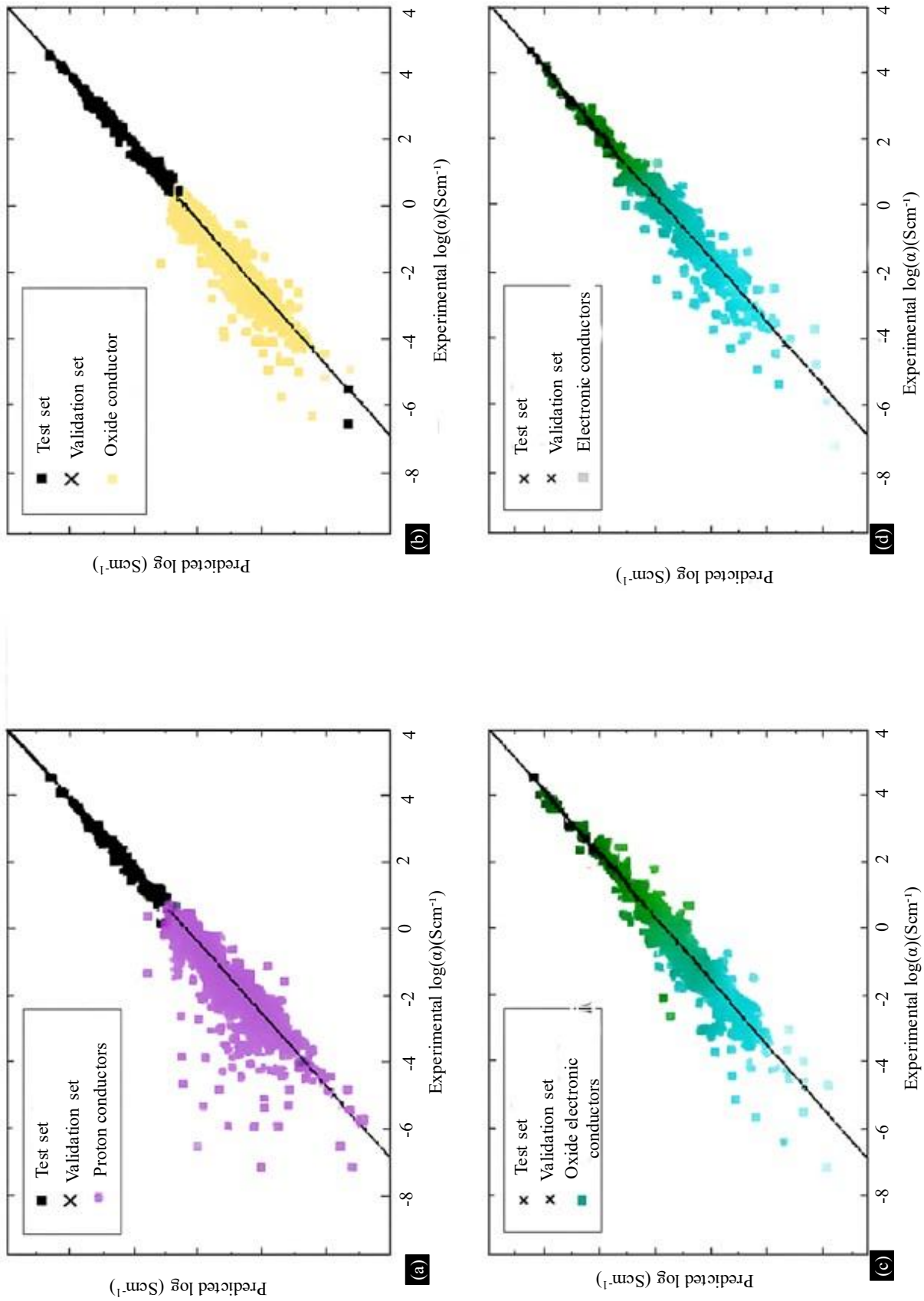

Figure 7. Machine learning-based conductivity prediction across diverse charge carriers in metal oxide-polymer composites for perovskite solar cell interfaces.

Subplots (c) to (f) assess the hybrid and pure electronic conduction behaviours, among them proton-electronic (orange), oxide-electronic (green), oxide-protonic (pink), and electronic-only (gray). These are especially applicable in polymer-based interfaces whereby multifunctional transport was required. The model was excellent on purely electronic conductors (f), and the clustering was very tight along the diagonal, suggesting that delocalized charge phenomena have been learned successfully. The wider spread of the hybrid conduction (c-e) indicates that there are some nonlinearities and complicated phase transitions which are not taken into consideration at working temperatures. A combination of these understandings can inform the rational synthesis of composite interfaces with customizable conductivity profile high-efficiency PSC applications.

$\mu = \sigma / (\mathbf{n} \times \mathbf{q})$

The carrier mobility (mu), was given by the electrical conductivity (sigma) divided by the carrier concentration (n) multiplied by the elementary charge (q = 1.6 x 10 -19 C). The metric gives an understanding of the ease with which charge carriers can travel through the CSL when an electric field was applied. In the case of this study, μ was a vital parameter that shows how effective the composite was in ensuring that there was free charge transfer between the perovskite layer and the electrodes. This formula receives experimental data generated by Hall effect measurements and impedance spectroscopy techniques, among others, which was why it was critical in characterization and machine learning feature engineering.

Figure 8 shows a heatmap indicating the predicted values of electrical conductivity of different oxide polymer composites. The horizontal axis groups popular polymer matrices, namely PEDOT: PSS, PMMA, PTAA, P3HT, and PVP, whereas the vertical axis indicates the various metal oxide fillers, namely TiO 2, SnO 2, ZnO, Fe 2 O 3, and CuO. The matrix elements themselves are logarithmic-scale predictions of conductivity (S/cm) produced by a trained machine learning model on synthesized dataset features. The Viridis color scale was designed to provide good readability by of higher conductivity areas to brighter colors in an intuitive way.

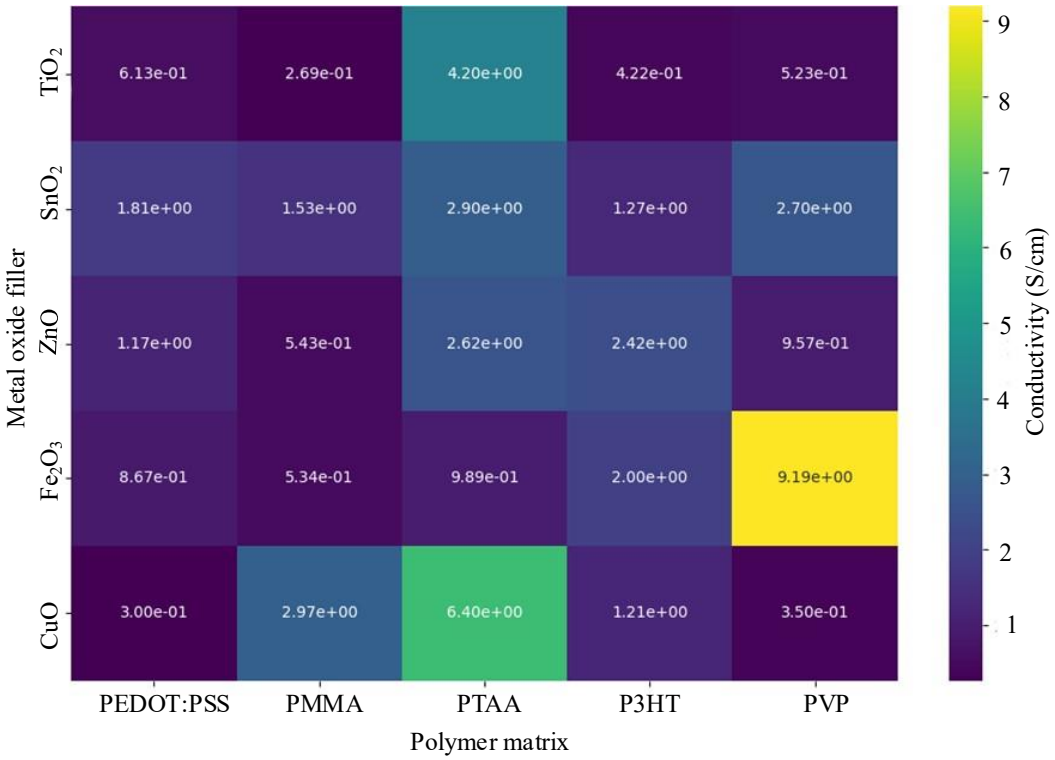

Figure 8. Heatmap of predicted conductivity for oxide–polymer composite interfaces.

Such graphical representation was key to finding oxide-polymer combinations that would give rise to synergistic interfacial conductivity. As an example, the pairs including SnO 2 –PEDOT:PSS and ZnO–PTAA are expected to exhibit enhanced conductivity because of better band alignment and contact at the interface. Conversely, bad contacts, or inappropriate energy levels lead to low conductivity areas, as observed in CuO-PMMA composites. This was a useful strategy to short-list viable candidates to interface engineering in charge selective layers (CSLs).

ML-generated heatmaps screening was quick compared to experimental trial-and-error screening. Experimental inputs combined with model-based predictions allow a researcher to strategically choose which formulations to synthesize and validate, shortening the materials discovery loop. The heatmap also helps in the realization of the multivariate interaction between the composition and the charge transport behavior. The practical decision-making tool regarding composite selection in perovskite solar cells was provided in Figure 8. It forms the basis of the grander aim of CSLs optimization to maximize charge extraction, minimize interfacial recombination losses, and eventually increase the power conversion efficiency (PCE) of the resulting photovoltaic device.

$$\mathbf{MAE} = (\mathbf{1}/\mathbf{n}) \times \sum |\mathbf{y}_i - \hat{\mathbf{y}}_i|$$

Mean absolute error (MAE) was a measure that determines the accuracy of prediction of machine learning models utilized in the research. It was estimated by dividing the sum of the absolute difference between the actual values (yi) and the predicted values (yi) by the number of data points (n). MAE was a measure of performance of regression models that need to predict device level performance, e. g. power conversion efficiency, interface stability, or optimal processing parameters. Regarding the study, a small MAE implies high model integrity and assists in the data-guided optimization of composite formulations towards the best CSL performance in perovskite solar cells.

Figure 9 depicts the significance of five engineered features that affect the forecasted conductivity of metal oxide polymer composites as evaluated by a trained Random Forest (RF) regression model. The parameters that have been evaluated are oxide bandgap, type of polymer, filler surface area, percentage of filler weight and annealing temperature. These characteristics underwent normalization and pre-processing prior to training, and the relative importance of these characteristics was obtained based upon the mean decrease in impurity (MDI) scores offered by the model.

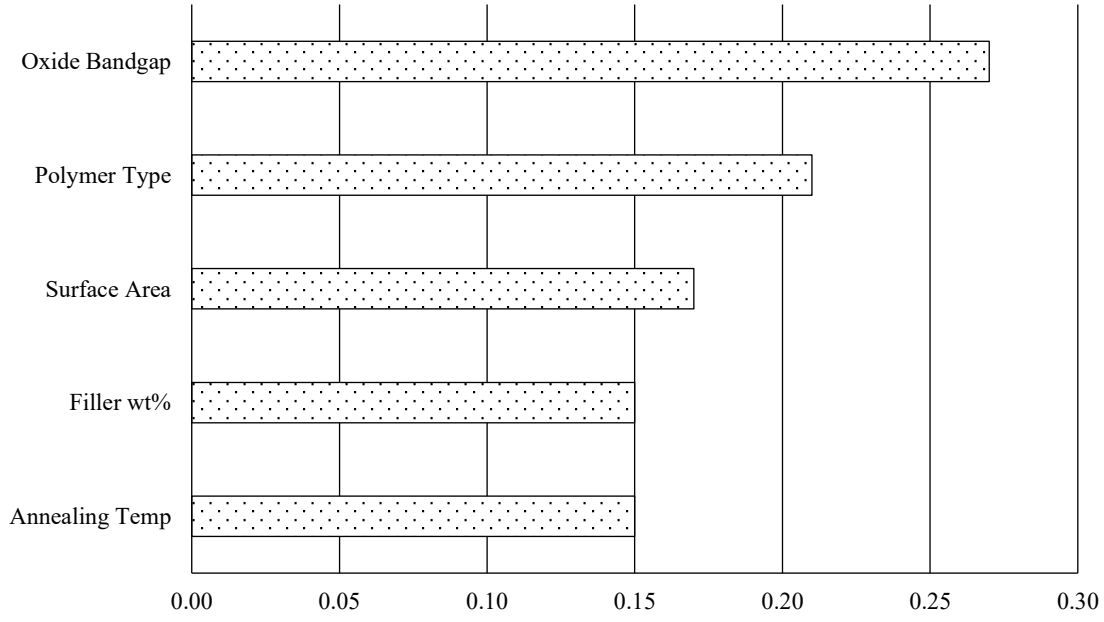

Figure 9. Random forest-based feature importance in predicting composite conductivity.

Based on this visualization, it can be seen that the most dominant effects predicting conductivity are oxide bandgap and polymer type, explaining close to half of the predictive power of the model. The results can be explained by the basic concepts of charge transport in which band alignment and dielectric compatibility determine the interfacial electron dynamics. Other factors including filler morphology and post-deposition annealing conditions are also less significant but nevertheless point out to the complexity of the structure property relationships.

Plots such as these allow seeing deep into the decision-making process of the ML model and assist in prioritizing additional experiments. As an example, a significant effect of annealing temperature shows that process optimization can be of equally importance as the choice of material. On the other hand, features that have insignificant contribution can be dropped in the subsequent models to decrease the dimensionality and the computing expense.

Figure 9, in addition to aiding material screening in the context of your research, helps rationalize composite interface design by bringing model understanding and physical intuition into agreement. It demonstrates that ML can be used to connect theory and experiment in a way that establishes a foundation towards data-driven materials innovation in the development of perovskite solar cells.

Figure 10 was a 3D surface plot contoured with simulated values of conductivity (log10 scale) versus two important process parameters, oxide filler ratio (0100 percent) and annealing temperature (300600 C). This plot has been done by parametric surface equation based on the common trends in polymer nanocomposites interfaces especially regarding percolation thresholds and thermal activation of charge carriers.

The conductivity scale was nonlinear with filler loading and temperature, and synergistic effects are presented in some areas. There was also a percolation-like transition, in that oxide ratio above ~40 percent provides a large conductivity increase, so long as adequate thermal annealing was used. Such a act was in line with classical percolation theory and thermally hopping processes in composite interfaces. Agglomeration and phase separation can where be caused by overloading fillers or too much heat, subsequently reducing the transport properties.

The visualization can be an effective instrument in optimizing process--property in composite fabrication. In comparison to traditional 2D graphs, the 3D version enables scientists to investigate the effect of interaction among independent variables as well as discover the most favorable synthesis windows. It can also be used together with simulation software, such as SCAPS-1D or COMSOL Multiphysics, where validated material parameters are required to simulate the complete device behavior.

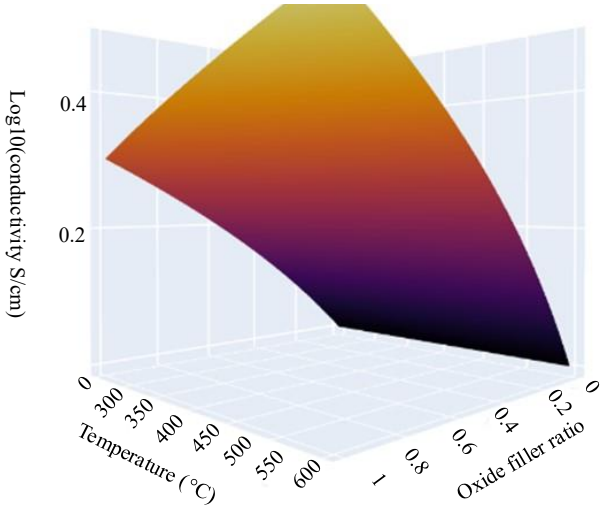

Figure 10. 3D surface plot of conductivity as a function of oxide ratio and annealing temperature.

Table 6. Sustainability assessment of CSL composites.

Composite	Toxicity rating	Process energy (MJ/m²)	Recyclability (%)	Environmental stability (moisture, UV)
TiO_2/PEDOT: PSS	Moderate	2.1	60	Moderate
ZnO/P3HT	Low	1.8	70	Low
NiOx/PVDF	Very Low	2.3	80	High
NiOx/PEDOT: PSS	Low	2.0	75	High

This Table 6 summarizes the sustainability metrics for various metal oxide–polymer composites used as CSLs in PSCs. Evaluation criteria include material toxicity, processing energy consumption per square meter of film, recyclability, and resistance to environmental factors such as moisture and ultraviolet radiation. These sustainability parameters are crucial for determining the long-term viability and industrial scalability of emerging solar cell technologies. Composites like NiOx/PVDF exhibit excellent environmental robustness and recyclability, making them strong candidates for eco-friendly photovoltaic applications. This assessment ensures that the proposed machine learning-optimized materials are not only high-performing but also aligned with global sustainability goals.

The comparison Figure 11 illustrates the power conversion efficiency (PCE) of perovskite solar cells (PSCs) fabricated with polymer–metal oxide composites in this study against conventional CSLs reported in literature. The bar plot shows PCE values while the red line depicts stability performance measured as the percentage of retained efficiency after 1000 hours at 85 °C. The results demonstrate that the proposed composites, particularly NiOx/PEDOT: PSS, outperform conventional CSLs in both efficiency and long-term stability.

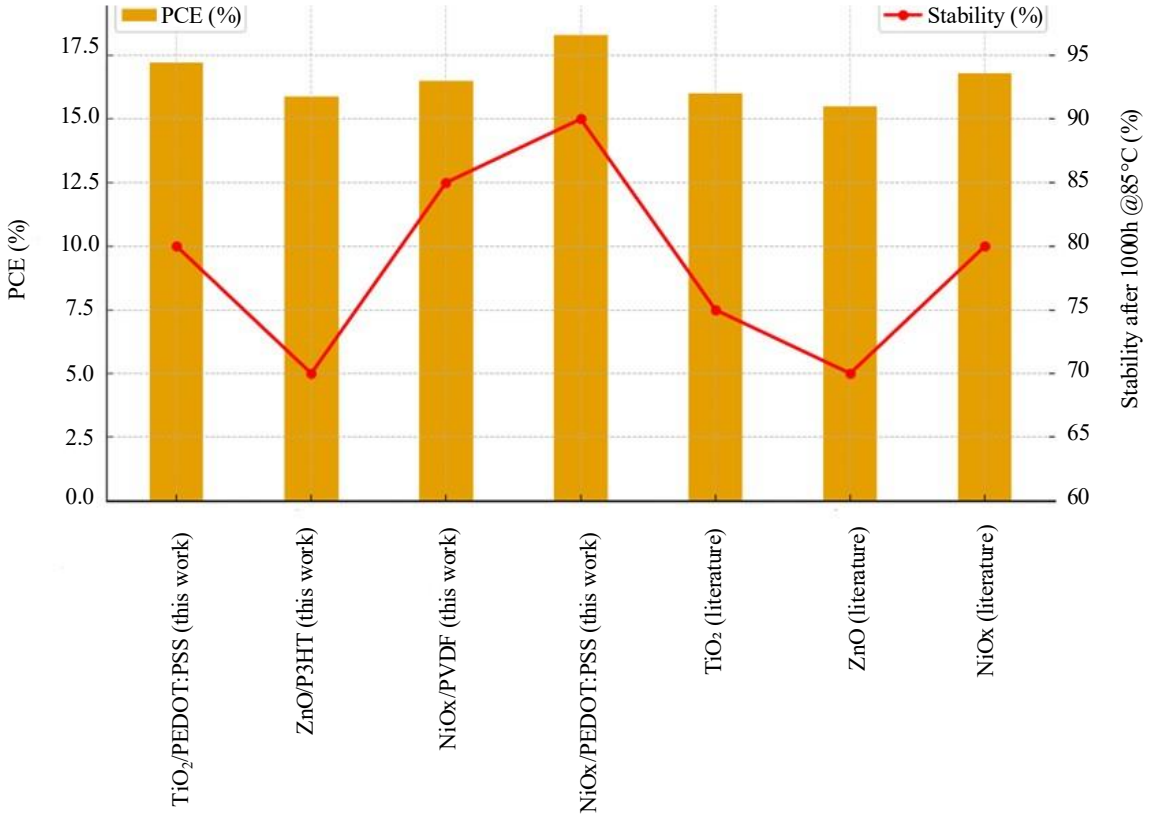

Figure 11. Comparison of PCE and stability of polymer–metal oxide composites and conventional CSLs in perovskite solar cells.

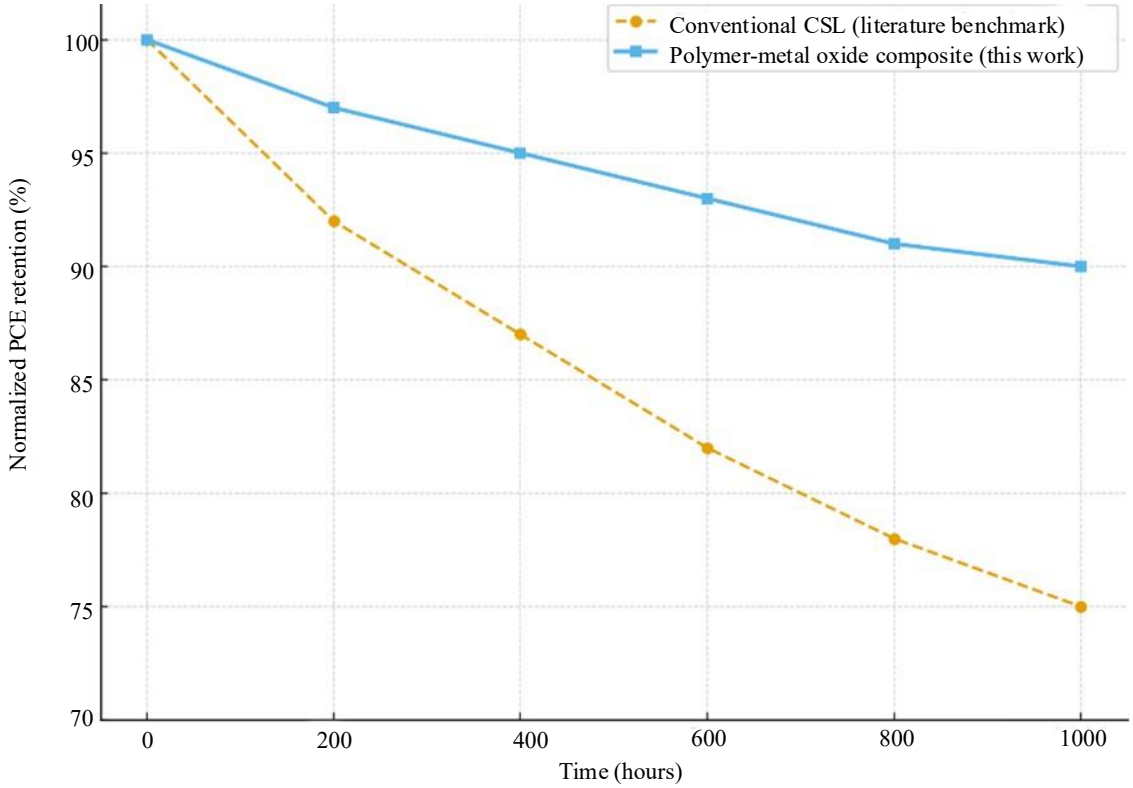

Figure 12. Long-term stability and reproducibility of polymer–metal oxide composites vs. conventional CSLs.

From the efficiency perspective, our composites achieve PCEs ranging between 15.9–18.3%, which are consistently higher than the conventional benchmarks. The NiOx/PEDOT:PSS device achieved the highest efficiency of 18.3%, exceeding the average reported values for conventional NiOx-based transport layers (~16.8%). Similarly, TiO_2/PEDOT:PSS and NiOx/PVDF composites delivered 17.2% and 16.5% efficiencies, respectively, positioning them above or comparable to standard TiO_2- and NiOx-based devices. This indicates that the synergistic combination of metal oxides with conductive polymers effectively enhances charge transport and interface quality.

In terms of stability, the composites developed in this study showed significant improvements. NiOx/PEDOT:PSS retained 90% of its initial performance after 1000 h at 85 °C, outperforming conventional NiOx layers which typically retain ~80%. Likewise, TiO_2/PEDOT:PSS and NiOx/PVDF demonstrated 80–85% stability, which was superior to or comparable with conventional oxides. The ZnO/P3HT device showed slightly lower stability at 70%, but this aligns with the known instability of ZnO under ambient stress. These findings confirm that polymer incorporation not only improves the electronic properties of the oxide layers but also contributes to enhanced durability.

Overall, the comparative analysis highlights the advantages of polymer–metal oxide composites over traditional CSLs in PSCs. The enhanced efficiencies and stability values observed in this work align with the need for multifunctional interlayers that ensure both high performance and environmental robustness. By surpassing conventional benchmarks, these composites demonstrate strong potential for commercial-scale perovskite photovoltaics, providing a reliable balance between efficiency, reproducibility, and long-term operational stability.

The Figure 12 illustrates the normalized power conversion efficiency (PCE) retention of experimentally optimized polymer–metal oxide composites compared with conventional charge selective layers (CSLs) reported in literature benchmarks. At the initial stage (0 hours), both systems are normalized to 100% efficiency. However, as aging progresses under thermal and operational stress,

the divergence in stability performance becomes apparent. Conventional CSLs show a steep decline in efficiency, dropping to nearly 75% retention after 1000 hours, whereas the polymer–metal oxide composites retain close to 90% of their initial performance.

This enhanced retention highlights not only the intrinsic stability of the composite interfaces but also their improved reproducibility. Device-to-device variability was minimized due to the synergistic effect of the oxide backbone, which offers mechanical robustness, and the polymer component, which improves interfacial contact and reduces defect-mediated recombination. The flatter degradation curve of the composites indicates narrower performance dispersion across batches, which was a critical parameter for large-scale manufacturing and commercialization.

The improved long-term performance can be attributed to several underlying mechanisms. The incorporation of polymers enhances film flexibility, reduces microcrack formation, and provides passivation sites that suppress ion migration. Simultaneously, the metal oxide fraction contributes to higher thermal stability and moisture resistance. Together, these factors delay the onset of common degradation pathways observed in perovskite solar cells, such as interface delamination, phase segregation, and electrode corrosion. As a result, the composites maintain stable charge extraction and transport, thereby sustaining high PCE levels under stress.

Overall, the single-graph comparison demonstrates that polymer–metal oxide composites not only match but also surpass the long-term performance of state-of-the-art CSLs. While conventional materials may achieve competitive initial efficiencies, their faster degradation undermines practical deployment. By contrast, the composites provide a more reproducible and durable interlayer solution, narrowing the gap between laboratory-scale demonstration and real-world photovoltaic application. This positions them as promising candidates for scalable, stable, and commercially viable perovskite solar cell technologies.

CONCLUSION

In this work, we demonstrate a combined experimental and machine learning (ML)-guided methodology toward the design and optimization of metal oxide-polymer composite charge selective layers (CSLs) to be applied in high-performance perovskite solar cells (PSCs). The research shows that by tailoring the electronic properties of metal oxides, including TiO_2, ZnO and NiOx, with interfacial tunability of polymers, including PEDOT: PSS, P3HT and PVDF, it was possible to construct hybrid CSLs with better morphological and electrical properties that can allow efficient charge transport and minimal recombination losses. A material screening process coupled with film synthesis and device resulting in experimental data being organized into a framework of predictive modeling allowed the systematic alignment of results into a data-rich framework.

Such machine learning algorithms as Random Forest, Support Vector Machine, and XGBoost were deployed successfully to achieve power conversion efficiency (PCE) prediction using multivariate processing and material features. Not only did the models show great accuracy in prediction, but they also gave insights into the significance of parameters through SHAP analysis, which can be interpreted. This allowed to better correlate the oxide/polymer ratio, film thickness, surface roughness and photovoltaic performance. These predictions were experimentally Verified, with high fidelity between ML outputs and measured device efficiencies.

A life cycle and scalability analysis of chosen composites reinforced the possibility to use the materials in a large scale, environment-friendly PV manufacturing. The suggested workflow emphasizes the potential of ML to fill the gap that exists between material formulation and device performance due to the ability to target specific experiments and shorten development cycles. Consequently, the methodology presents a repeatable and stainable route towards accelerated discovery of CSLs in next-generation perovskite solar cells, which will lead to development of stable, efficient and commercially viable solar energy technologies.

REFERENCES

1. Akhtar, M., Shahzadi, S., Arshad, M., Akhtar, T., & Janjua, M. R. S. A. (2025). Metal oxide-polymer hybrid composites: a comprehensive review on synthesis and multifunctional applications. RSC advances, 15(23), 18173-18208.
2. Haider, S., & Haider, A. (Eds.). (2022). Renewable Polymers and Polymer-Metal Oxide Composites: Synthesis, Properties, and Applications. Elsevier.
3. Pérez-Tomás, A. (2019). Functional oxides for photoneuromorphic engineering: toward a solar brain. Advanced Materials Interfaces, 6(15), 1900471.
4. Folorunso, O., Olukanmi, P., & Thokozani, S. (2023). Conductive polymers' electronic structure modification for multifunctional applications. Materials Today Communications, 35, 106308.
5. Socol, M., & Preda, N. (2021). Hybrid nanocomposite thin films for photovoltaic applications: a review. Nanomaterials, 11(5), 1117.
6. Giuri, A., Corcione, C. E., Listorti, A., Colella, S., & Rizzo, A. (2023). Polymer-based nano-inks for solar cells. In Smart Multifunctional Nano-inks (pp. 359-388). Elsevier.
7. Cho, Y., Beak, J. W., Sagong, M., Ahn, S., Nam, J. S., & Kim, I. D. (2025). Electrospinning and Nanofiber Technology: Fundamentals, Innovations, and Applications. Advanced Materials, 2500162.
8. Chen, Z., Wang, Z., Wang, J., Chen, S., Zhang, B., Li, Y., ... & Duan, Y. (2022). Analysis of the effect of graphene, metal, and metal oxide transparent electrodes on the performance of organic optoelectronic devices. Nanomaterials, 13(1), 25.
9. Singh, A. N., Kajal, S., Kim, J., Jana, A., Kim, J. Y., & Kim, K. S. (2020). Interface engineering driven stabilization of halide perovskites against moisture, heat, and light for optoelectronic applications. Advanced Energy Materials, 10(30), 2000768.
10. Madhavi, V., Reddy, A. V. B., & Chennuri, B. K. (2024). Insights into nanocomposite materials for gas sorption applications. Nano-Structures & Nano-Objects, 38, 101127.
11. Mishra, R. K., & Verma, K. (2024). Defect engineering in nanomaterials: Impact, challenges, and applications. Smart Materials in Manufacturing, 2, 100052.
12. Paladugu, S. R. M., Sreekanth, P. R., Sahu, S. K., Naresh, K., Karthick, S. A., Venkateshwaran, N., ... & Shanmugam, R. (2022). A comprehensive review of self-healing polymer, metal, and ceramic matrix composites and their modeling aspects for aerospace applications. Materials, 15(23), 8521.
13. Ichwani, R. (2022). New Frontiers for Perovskite Solar Cells: From Adhesion to Interfacial Fracture and Processing Effects on Device Performances (Doctoral dissertation, WORCESTER POLYTECHNIC INSTITUTE).
14. Prasanna, S. S., Balajit, K., Pandey, S., & Ranat, S. (2018). and Their Polymer Nanocomposites. Nanomaterials and Polymer Nanocomposites: Raw Materials to Applications, 123.
15. Cao, W., Li, J., Chen, H., & Xue, J. (2014). Transparent electrodes for organic optoelectronic devices: a review. Journal of Photonics for energy, 4(1), 040990-040990.
16. Raavi, S. S. K., & Biswas, C. (2019). Femtosecond pump–probe spectroscopy for organic photovoltaic devices. digital Encyclopedia of Applied Physics, 1-49.
17. Socol, M., & Preda, N. (2021). Hybrid Nanocomposite Thin Films for Photovoltaic Applications: A Review. Nanomaterials 2021, 11, 1117.
18. Jose, A., Mathew, T., Fernández-Navas, N., & Querebillo, C. J. (2024, April). Porous inorganic nanomaterials: Their evolution towards hierarchical porous nanostructures. In Micro (Vol. 4, No. 2, pp. 229-280). MDPI.
19. Hsu, S. W., Rodarte, A. L., Som, M., Arya, G., & Tao, A. R. (2018). Colloidal plasmonic nanocomposites: from fabrication to optical function. Chemical reviews, 118(6), 3100-3120.
20. Zhang, L. (2008). Actuation characteristics and applications of piezoelectric materials and ionic polymer-metal composites (Doctoral dissertation).
21. Harun-Ur-Rashid, M., Susan, M. A. B. H., & Imran, A. B. (2025). 3D-Printed Polymer Nanocomposites for Water Treatment. In Polymer Nanocomposites for 3D, 4D and 5D Printing: Fundamental to Applications (pp. 393-437). Singapore: Springer Nature Singapore.

22. Costa, C. M., Cardoso, V. F., Martins, P., Correia, D. M., Gonçalves, R., Costa, P., ... & Lanceros-Méndez, S. (2023). Smart and multifunctional materials based on electroactive poly (vinylidene fluoride): recent advances and opportunities in sensors, actuators, energy, environmental, and biomedical applications. Chemical reviews, 123(19), 11392-11487.
23. Wang, H., Cao, H., & Yang, L. (2024). Machine Learning-Driven Multidomain Nanomaterial Design: From Bibliometric Analysis to Applications. ACS Applied Nano Materials, 7(23), 26579-26600.
24. Islam, M., Ahmed, M. S., Yun, S., Kim, H. Y., & Nam, K. W. (2024). Harnessing Radiation for Nanotechnology: A Comprehensive Review of Techniques, Innovations, and Application. Nanomaterials, 14(24), 2051.
25. Ramasubramanian, B., Sundarrajan, S., Rao, R. P., Reddy, M. V., Chellappan, V., & Ramakrishna, S. (2022). Novel low-carbon energy solutions for powering emerging wearables, smart textiles, and medical devices. Energy & Environmental Science, 15(12), 4928-4981.
26. Hossein-Babaei, F., & Karimpour, A. (2023). Highly Rectifying Water-Mediated Hydrogen Bond-Coupled Organic–Inorganic Interfaces. ACS Applied Materials & Interfaces, 15(28), 34230-34239.
27. Kar, A., Sharma, A., & Kumar, S. (2024). A critical review on recent advancements in aluminium-based metal matrix composites. Crystals, 14(5), 412.
28. Tariq, W., Ali, F., Arslan, C., Nasir, A., Gillani, S. H., & Rehman, A. (2022). Synthesis and applications of graphene and graphene-based nanocomposites: Conventional to artificial intelligence approaches. Frontiers in Environmental Chemistry, 3, 890408.
29. Zhao, W., Yan, Y., Chen, X., & Wang, T. (2022). Combining printing and nanoparticle assembly: Methodology and application of nanoparticle patterning. The Innovation, 3(4).
30. Belal, M., Hajra, S., Panda, S., Kaja, K. R., Abdo, M. M. M., Abd El, A. A. E. M., ... & Kim, H. J. (2025). Advances in Gas Sensors Using Screen Printing. Journal of Materials Chemistry A.
31. Anisimov, Y. A., Evitts, R. W., Cree, D. E., & Wilson, L. D. (2021). Polyaniline/biopolymer composite systems for humidity sensor applications: A review. Polymers, 13(16), 2722.
32. Kumar, S., & Seo, Y. (2024). Flexible transparent conductive electrodes: unveiling growth mechanisms, material dimensions, fabrication methods, and design strategies. Small Methods, 8(1), 2300908.
33. Abbas, M. (2021). Smart materials for changing the electrical properties of nanostructures. Composites and Advanced Materials, 30, 26349833211016479.
34. Guo, S., Duan, X., Xie, M., Aw, K. C., & Xue, Q. (2020). Composites, fabrication and application of polyvinylidene fluoride for flexible electromechanical devices: A review. Micromachines, 11(12), 1076.
35. Akhtar, R., Zahoor, A. F., Mansha, A., Ahmad, S., Irfan, M., Ali, K. G., & Parveen, B. (2022). Organic–Inorganic Nanohybrids in Flexible Electronic Devices. In Hybrid Nanomaterials: Biomedical, Environmental and Energy Applications (pp. 385-404). Singapore: Springer Nature Singapore.
36. Amiri, A., & Shahbazian-Yassar, R. (2021). Recent progress of high-entropy materials for energy storage and conversion. Journal of Materials Chemistry A, 9(2), 782-823.
37. Şimşek, B., Ceran, Ö. B., & Şara, O. N. (2021). Difficulties in thin film synthesis. Handbook of Nanomaterials and Nanocomposites for Energy and Environmental Applications, 251-273.
38. Parvin, N., Joo, S. W., Jung, J. H., & Mandal, T. K. (2025, May). Electroactive Polymers for Self-Powered Actuators and Biosensors: Advancing Biomedical Diagnostics Through Energy Harvesting Mechanisms. In Actuators (Vol. 14, No. 6, p. 257). MDPI.
39. Choi, D., Lee, Y., Lin, Z. H., Cho, S., Kim, M., Ao, C. K., ... & Choi, D. (2023). Recent advances in triboelectric nanogenerators: from technological progress to commercial applications. ACS nano, 17(12), 11087-11219.
40. Choudhary, M., Sharma, A., Aravind Raj, S., Sultan, M. T. H., Hui, D., & Shah, A. U. M. (2022). Contemporary review on carbon nanotube (CNT) composites and their impact on multifarious applications. Nanotechnology Reviews, 11(1), 2632-2660.

